Inorganic Chemistry
Communication

Inorg. Chem. **2010**, *49*, 6399–6401 **6399**
DOI: 10.1021/ic100945n

Reversible Apical Coordination of Imidazole between the Ni(III) and Ni(II) Oxidation States of a Dithiolate Complex: A Process Related to the Ni Superoxide Dismutase

Marcello Gennari,[†] Maylis Orio,[‡] Jacques Pécaut,[§] Frank Neese,[‡] Marie-Noëlle Collomb,[†] and Carole Duboc*[,†]

[†]*Université Joseph Fourier Grenoble 1/CNRS, Département de Chimie Moléculaire, UMR-5250, 38041 Grenoble Cedex 9 France,* [‡]*Institute for Physical and Theoretical Chemistry Universität Bonn, Wegelerstrasse 12, D-53113 Bonn, Germany, and* [§]*Laboratoire de Reconnaissance Ionique et Chimie de Coordination, UMR-E 3 CEA-UJF, 38054 Grenoble Cedex 09, France*

Received May 12, 2010

A bisamine aliphatic dithiolate $[Ni^{II}N_2S_2]$ complex that does yield a metal-based oxidation has been synthesized. A square pyramidal $[Ni^{III}N_3S_2]^+$ complex is generated by electrochemical oxidation in the presence of imidazole, mimicking the redox structural changes of NiSOD. In addition, EPR measurements coupled to DFT calculations demonstrate that the metal character in the redox active orbital increases drastically upon imidazole binding, implicating that these geometrical modifications are crucial for the stabilization of the Ni^{III} state.

Superoxide dismutases (SODs) serve a key antioxidant role in the protection of living cells against oxidative damage caused by the superoxide radical anion ($O_2^{\bullet -}$). This highly reactive oxygen species is destroyed by the SODs via disproportionation into hydrogen peroxide and molecular dioxygen.[1] Nickel-containing superoxide dimutases (NiSODs) are the most recently discovered SODs.[2] During catalysis, the Ni ion cycles between the +II and +III oxidation states.[3] In the reduced state, the Ni^{II} center is in a square planar $[N_2S_2]^{3-}$ environment with two thiolates from cysteines, one N-amidate from the peptide backbone, and the N-terminal amino group.[4,5] Upon oxidation, the Ni site is converted to a $[N_3S_2]$ square pyramid via the coordination of an axial N-imidazole ligand derived from a histidine. This unusual redox-state-dependent change in metal coordination number is crucial for SOD activity since mutations of the axial histidine lead to a drastic decrease of the enzyme reactivity.[6]

It has been shown that synthetic square planar bisamide aliphatic dithiolate $[Ni^{III}N_2S_2]^-$ model complexes can generate square pyramidal Ni^{III} compounds via the axial coordination of a pyridine ligand in the presence of a large excess of pyridine.[7−10] Nevertheless, neither the reversibility of this process nor the role of this apical coordination on the electronic structure of the Ni ion has been investigated in detail. Another unique feature of the NiSOD active site is the amide/amine coordination motif. Its role in the catalytic mechanism is to protect the thiolate ligands against oxidative damage[7] by ensuring a Ni-based oxidation process.[11−13] It was commonly admitted that synthetic bisamine $[Ni^{II}N_2S_2]$ complexes have a propensity to undergo oxidation at the thiolate ligands and not at the Ni center,[14−16] in contrast to bisamide or monoanionic compounds.[7−10] Here, we report on the first bisamine dithiolate $[Ni^{II}N_2S_2]$ complex that does yield a metal-based oxidation. Even more interestingly, an electrochemical investigation shows the reversible, oxidation-state-dependent generation of a square pyramidal $[Ni^{III}N_3S_2]^+$ complex in the presence of imidazole. In addition, EPR measurements coupled to DFT calculations demonstrate that the nickel character in the redox active orbital increases drastically upon imidazole binding. Finally, although this diamine Ni^{II} complex does not mimic the mixed amide/amine coordination sphere of the NiSOD, it replicates some of its structural, dynamic, and redox properties.

*To whom correspondence should be addressed. E-mail: carole.duboc@ujf-grenoble.fr.

(1) Miller, A. F. *Curr. Opin. Chem. Biol.* **2004**, *8*, 162–168.
(2) Youn, H.-D.; Kim, E.-J.; Roe, J.-H.; Hah, Y. C.; Kang, S.-O. *Biochem. J.* **1996**, *318*, 889–896.
(3) Choudhury, S. B.; Lee, J. W.; Davidson, G.; Yim, Y. I.; Bose, K.; Sharma, M. L.; Kang, S. O.; Cabelli, D. E.; Maroney, M. J. *Biochemistry* **1999**, *38*, 3744–3752.
(4) Barondeau, D. P.; Kassmann, C. J.; Bruns, C. K.; Tainer, J. A.; Getzoff, E. D. *Biochemistry* **2004**, *43*, 8038–8047.
(5) Wuerges, J.; Lee, J.-W.; Yim, Y.-I.; Yim, H.-S.; Kang, S.-O.; Djinovic Carugo, K. *Proc. Natl. Acad. Sci. U.S.A.* **2004**, *101*, 8569–8574.
(6) Bryngelson, P. A.; Arobo, S. E.; Pinkham, J. L.; Cabelli, D. E.; Maroney, M. J. *J. Am. Chem. Soc.* **2004**, *126*, 460–461.
(7) Fiedler, A. T.; Bryngelson, P. A.; Maroney, M. J.; Brunold, T. C. *J. Am. Chem. Soc.* **2005**, *127*, 5449–5462.
(8) Kruger, H. J.; Holm, R. H. *Inorg. Chem.* **1987**, *26*, 3645–3647.
(9) Kruger, H. J.; Peng, G.; Holm, R. H. *Inorg. Chem.* **1991**, *30*, 734–742.
(10) Hanss, J.; Kruger, H. J. *Angew. Chem., Int. Ed.* **1998**, *37*, 360–363.
(11) Shearer, J.; Zhao, N. *Inorg. Chem.* **2006**, *45*, 9637–9639.
(12) Shearer, J.; Dehestani, A.; Abanda, F. *Inorg. Chem.* **2008**, *47*, 2649–2660.
(13) Mullins, C. S.; Grapperhaus, C. A.; Kozlowski, P. M. *J. Biol. Inorg. Chem.* **2006**, *11*, 617–625.
(14) Mills, D. K.; Reibenspies, J. H.; Darensbourg, M. Y. *Inorg. Chem.* **1990**, *29*, 4364–4366.
(15) Colpas, G. J.; Kumar, M.; Day, R. O.; Maroney, M. J. *Inorg. Chem.* **1990**, *29*, 4779–4788.
(16) Grapperhaus, C. A.; Maguire, M. J.; Tuntulani, T.; Darensbourg, M. Y. *Inorg. Chem.* **1997**, *36*, 1860–1866.

Published on Web 06/16/2010

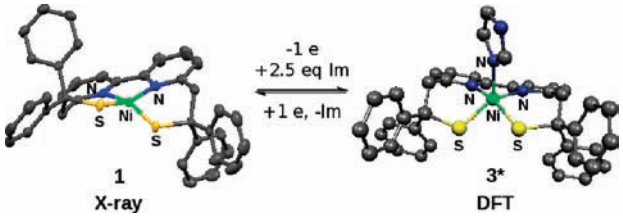

Figure 1. Redox equilibrium between **1** (X-ray structure with 50% thermal ellipsoids and H atoms omitted) and **3*** (optimized structure; Im=imidazole). Selected bond distances in **1** (Å): Ni(1)−S(1)= 2.1732(6), Ni(1)−S(2)=2.1759(6), Ni(1)−N(1)=1.9345(16), Ni(1)−N(2)= 1.9352(16).

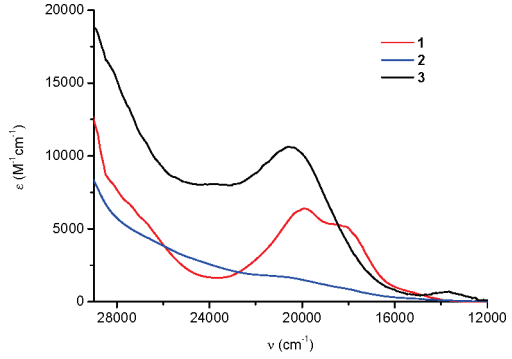

Figure 2. Electronic absorption spectra of **1**, **2**, and **3** in CH_2Cl_2, 0.1 M Bu_4NPF_6.

The disodium salt of the ligand LH_2 (2,2′-(2,2′-bipyridine-6,6′-diyl)bis(1,1-diphenylethanethiol))[17] reacts in THF with $NiCl_2 \cdot 6H_2O$, leading to a purple precipitate corresponding to [NiL] (**1**). The mononuclear structure of the complex is evidenced by the X-ray analysis of single crystals (Figures 1 and S1, Supporting Information).

The Ni^{II} ion is contained within a distorted square plane with two N amine and two S thiolate atoms of L^{2-} as ligands, characterized by a pseudotetrahedral twist angle (S−Cu−S/N−Cu−N) of 29.15°. The Ni−N/S distances lie in the range found in related bisamine $[Ni^{II}N_2S_2]$ complexes[14−16,18] and compare well with the reduced state of the NiSOD (Ni−N_{amine}: 1.87(6) Å and Ni−$S_{trans/amine}$: 2.16(2) Å; Table S2, Supporting Information).[4,5]

The electronic absorption spectrum of a violet CH_2Cl_2 solution of **1** displays two low energy bands at 18 000 and 19 700 cm^{-1} (Figure 2), characteristic for such systems.[19] TD-DFT calculations further confirm the presence of two main electronic transitions (Figure S9, Table S8, Supporting Information) that can be assigned to the S(π)/Ni(π) → Ni($d_{x^2-y^2}$) and Ni(d_{z^2}) → Ni ($d_{x^2-y^2}$) transitions, respectively. A good agreement is obtained when comparing the experimental and computed energies of the electronic excitations, and the latter assignment is also consistent with previous studies on bisamine $[Ni^{II}N_2S_2]$ complexes.[12] Furthermore, the low spin character of the Ni^{II} ion in **1** has been evidenced by a diamagnetic ^1H NMR spectrum. These data demonstrate that the square planar geometry of the Ni center remains in solution.

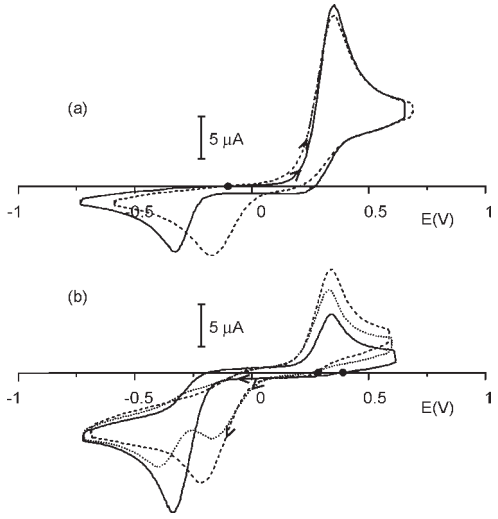

Figure 3. Cyclic voltammograms of a 1.6 mM solution of **1** in CH_2Cl_2, 0.1 M Bu_4NPF_6 at a vitreous carbon electrode (3 mm in diameter), (a) in the presence (dashed line) or the absence (solid line) of imidazole (2.5 equiv) and (b) after exhaustive electrolysis at +0.38 V (0.94 electron per molecule of **1** involved; solid line) followed by the addition of 1 equiv (dotted line) and 2.5 equiv (dashed line) of imidazole. Potentials are referred to a Ag/Ag^+ (10 mM $AgNO_3$) reference electrode in CH_3CN, 0.1 M Bu_4NClO_4. Scan rate of 100 mVs^{-1}.

The electrochemical behavior of **1** has been investigated in CH_2Cl_2 under argon (Figure 3 and Figures S2 and S3, Supporting Information). The cyclic voltammogram displays two one-electron metal-based processes: a quasi-reversible Ni^{II}/Ni^{I} reduction wave at $E_{1/2}$ = −1.68 V vs Ag/Ag^+ and an irreversible Ni^{III}/Ni^{II} oxidation peak at E_{pa} = +0.34 V. The $[Ni^{III}L]^+$ complex undergoes a fast chemical reaction as evidenced by the appearance on the reverse scan of an irreversible reduction peak at E_{pc} = −0.34 V, corresponding to the reduction of the newly formed species. A bulk electrolysis experiment carried out at E = +0.38 V leads to a stable EPR-silent, light orange solution (Figure 2) corresponding to the almost quantitative formation of a Ni^{III} dimer (**2**). Indeed, the ESI mass spectrum of a chemically generated solution of **2** (Figure S4, Supporting Information) reveals a fragment at m/z = 1309 corresponding to $[Ni_2L_2Cl]^+$. Such dimerization processes have already been observed upon the oxidation of mononuclear bisamide $[Ni^{II}N_3S_2]^{2-}$ complexes,[9] and a structure has been proposed on the basis of a computational analysis of viable dimer models.[20] During the oxidation process, the transient formation of a Ni^{II}-thiyl radical species, which undergoes a dimerization involving the formation of a S−S bond, cannot be fully excluded. However, such a process has only been observed with aromatic thiolate ligands that stabilize radical species.[21]

The addition of up to 2.5 equiv of imidazole in an electrogenerated solution of **2** leads to the progressive appearance of a new irreversible reduction peak at E_{pc} = −0.20 V at the expense of that located at E_{pc} = −0.34 V (Figure 3b). The resulting red solution displays a rhombic EPR S = 1/2 signal (Figure 4). The three-line superhyperfine pattern in the g_z component is assigned to a single nitrogen donor atom ($^{15}I_N$ = 1) arising from an imidazole ligand axially bound to

(17) Kopf, M. A.; Varech, D.; Tuchagues, J. P.; Mansuy, D.; Artaud, I. *J. Chem. Soc., Dalton Trans.* **1998**, 991–998.
(18) Ma, H.; Chattopadhyay, S.; Petersen, J. L.; Jensen, M. P. *Inorg. Chem.* **2008**, *47*, 7966–7968.
(19) Maroney, M. J.; Choudhury, S. B.; Bryngelson, P. A.; Mirza, S. A.; Sherrod, M. J. *Inorg. Chem.* **1996**, *35*, 1073–1076.
(20) Fiedler, A. T.; Brunold, T. C. *Inorg. Chem.* **2007**, *46*, 8511–8523.
(21) Stenson, P. A.; Board, A.; Marin-Becerra, A.; Blake, A. J.; Davies, E. S.; Wilson, C.; McMaster, J.; Schroder, M. *Chem.—Eur. J.* **2008**, *14*, 2564–2576.

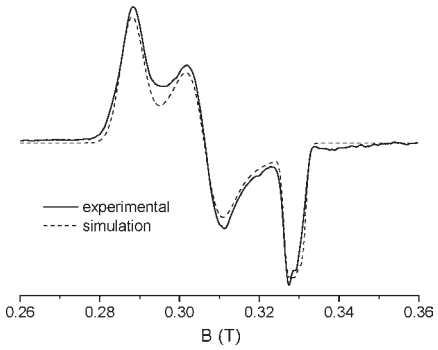

Figure 4. X-band EPR spectrum of **3** obtained after the addition of 2.5 equiv of imidazole in electrogenerated **2**, recorded in CH2Cl2 (0.1 M Bu_4NPF_6) at 100 K. Parameters used for the simulation: $g_x = 2.315$, $g_y = 2.177$, $g_z = 2.029$, and $A_z = 54$ MHz.

the Ni ion. A similar spectrum has been obtained in the presence of pyridine (Figure S6, Supporting Information). The comparison of the EPR parameters of these two mononuclear Ni^{III} complexes with those of previously reported $[Ni^{III}(N_{amide})_2N_{pyridine}S_2]^-$ complexes[7−10,22] (Table S3, Supporting Information) are consistent with the formation of a mononuclear square pyramidal low spin Ni^{III} complex $[NiL(imidazole)]^+$, **3**, with a d_{z^2} ground state. The absorption spectrum of **3** displays two visible features at 13 700 and 20 500 cm^{-1} assigned to $Ni(z^2) \rightarrow Ni(x^2 - y^2)$ and $S(\pi) \rightarrow Ni(\sigma)$ CT transitions, respectively (Figure 2).[7]

Species **3** can also be generated via bulk electrolysis at +0.38 V of **1** in the presence of 2.5 equiv of imidazole (Figure S2, Supporting Information). The exhaustive reduction of **3** at −0.4 V regenerates **1** with a yield of 85%, demonstrating the reversibility of the coordination process of imidazole (Figure S2).

A DFT geometry optimization has been carried out on complex **1**, yielding reasonably accurate Ni^{II}−S/N bond lengths (2.180 and 1.918 Å, respectively) compared to the experimental ones (Table S7, Supporting Information). Starting from the optimized structure of **1**, the optimized structures of $[NiL]^+$, which correspond to the monomeric form of the dimer **2**, and of **3**, named **3***, have been calculated (Figures 1 and S8, Supporting Information). The computed Ni−S/N distances (2.14−2.26 and 1.95−1.99 Å, respectively) are consistent with a Ni^{III} species (Table S7, Supporting Information).[4,7,10] In the case of $[NiL]^+$, the redox-active orbital is primarily localized on the metal center (42% on Ni vs 24% on each S; Table 1). The imidazole coordination in **3*** increases the spin population on Ni from 49% to 82%. The same analysis applies when comparing the metal character of the redox-active MOs (76% in **3*** vs 42% in $[NiL]^+$). Clearly, the conversion of a square planar geometry to a square pyramidal environment drastically stabilizes the Ni^{III} state. Moreover, the computed EPR parameters for **3*** ($g_x = 2.252$, $g_y = 2.199$, $g_z = 2.071$, and $A_z = 53$ MHz) agree reasonably well with the experimental data, thus validating our theoretical approach.

Table 1. Composition of the Redox-Active MO and Mulliken Spin Populations Obtained from DFT Calculations on Complexes $[NiL]^+$ and **3***

	MO comp. (%)[a]			Mulliken spin pop.		
	Ni	S	S′	Ni	S	S′
$[NiL]^+$	42.1	24.1	24.2	0.49	0.24	0.25
3*	75.9	1.8	12.5	1.07	−0.09	−0.14

[a] Ni, 3d, 4s, and 4p and S, 3s, 3p, and 3d contribution.

Complex **1** does not display SOD activity using the xanthine/xanthine oxidase assay[23] in the presence or in the absence of imidazole. This lack of activity has been also reported for all of the tested synthetic bisamine,[24] bisamide,[24,25] and mixed amide/amine[11,26] dithiolate Ni^{II} complexes. So far, SOD activity has only been reported for metallopeptide-based models[27,28] and one synthetic $[Ni^{II}N_3S]^+$ complex.[25]

In conclusion, we have demonstrated that a neutral bisamine aliphatic dithiolate Ni^{II} complex does yield metal-based oxidation, contrary to widespread belief. This system mimics the structural changes observed during the NiSOD catalytic cycle since the binding of imidazole upon oxidation of the Ni ion is reversible. In addition, DFT calculations provide evidence that these geometrical modifications are crucial to stabilizing the Ni^{III} state.

Supporting Information Available: Synthetical procedure and cif file of **1**, mass spectrometry of **2**, additional data on the electrochemical and EPR properties and the DFT investigation of **1**−**3**. This material is free of charge via the Internet at http://pubs.acs.org.

(22) Green, K. N.; Brothers, S. M.; Jenkins, R. M.; Carson, C. E.; Grapperhaus, C. A.; Darensbourg, M. Y. *Inorg. Chem.* **2007**, *46*, 7536–7544.
(23) Tabbi, G.; Driessen, W. L.; Reedijk, J.; Bonomo, R. P.; Veldman, N.; Spek, A. L. *Inorg. Chem.* **1997**, *36*, 1168–1175.
(24) Shearer, J.; Long, L. M. *Inorg. Chem.* **2006**, *45*, 2358–2360.
(25) Jenkins, R. M.; Singleton, M. L.; Almaraz, E.; Reibenspies, J. H.; Darensbourg, M. Y. *Inorg. Chem.* **2009**, *48*, 7280–7293.
(26) Gale, E. M.; Patra, A. K.; Harrop, T. C. *Inorg. Chem.* **2009**, *48*, 5620–5622.
(27) Shearer, J.; Neupane, K. P.; Callan, P. E. *Inorg. Chem.* **2009**, *48*, 10560–10571.
(28) Krause, M. E.; Glass, A. M.; Jackson, T. A.; Laurence, J. S. *Inorg. Chem.* **2009**, *49*, 362–364.